



TITLE:

Noncontact Respiratory Measurement for Multiple People at Arbitrary Locations Using Array Radar and Respiratory-Space Clustering

AUTHOR(S):

Koda, Takato; Sakamoto, Takuya; Okumura, Shigeaki; Taki, Hirofumi

CITATION:

Koda, Takato ...[et al]. Noncontact Respiratory Measurement for Multiple People at Arbitrary Locations Using Array Radar and Respiratory-Space Clustering. IEEE Access 2021, 9: 106895-106906

ISSUE DATE:

2021

URL:

<http://hdl.handle.net/2433/277783>

RIGHT:

This work is licensed under a Creative Commons Attribution-NonCommercial-NoDerivatives 4.0 License.

Received July 12, 2021, accepted July 20, 2021, date of publication July 26, 2021, date of current version August 5, 2021.

Digital Object Identifier 10.1109/ACCESS.2021.3099821

Noncontact Respiratory Measurement for Multiple People at Arbitrary Locations Using Array Radar and Respiratory-Space Clustering

TAKATO KODA¹, TAKUYA SAKAMOTO¹, (Senior Member, IEEE), SHIGEAKI OKUMURA², AND HIROFUMI TAKI², (Member, IEEE)

¹Department of Electrical Engineering, Graduate School of Engineering, Kyoto University, Kyoto 615-8510, Japan

²MaRI Company Ltd., Kyoto 600-8815, Japan

Corresponding author: Takuya Sakamoto (sakamoto.takuya.8n@kyoto-u.ac.jp)

This work was supported in part by the JSPS KAKENHI under Grant 19H02155, in part by the JST PRESTO under Grant JPMJPR1873, and in part by the JST COI under Grant JPMJCE1307.

This work involved human subjects or animals in its research. Approval of all ethical and experimental procedures and protocols was granted by the Ethics Committee of the Graduate School of Engineering, Kyoto University, under Approval No. 201916.

ABSTRACT We developed a noncontact measurement system for monitoring the respiration of multiple people using millimeter-wave array radar. To separate the radar echoes of multiple people, conventional techniques cluster the radar echoes in the time, frequency, or spatial domain. Focusing on the measurement of the respiratory signals of multiple people, we propose a method called respiratory-space clustering, in which individual differences in the respiratory rate are effectively exploited to accurately resolve the echoes from human bodies. The proposed respiratory-space clustering can separate echoes, even when people are located close to each other. In addition, the proposed method can be applied when the number of targets is unknown and can accurately estimate the number and positions of people. We perform multiple experiments involving five or seven participants to verify the performance of the proposed method, and quantitatively evaluate the estimation accuracy for the number of people and the respiratory intervals. The experimental results show that the average root-mean-square error in estimating the respiratory interval is 196 ms using the proposed method. The use of the proposed method, rather the conventional method, improves the accuracy of the estimation of the number of people by 85.0%, which indicates the effectiveness of the proposed method for the measurement of the respiration of multiple people.

INDEX TERMS Antenna arrays, biomedical engineering, clustering methods, Doppler radar, MIMO radar, radar measurements, radar imaging, radar signal processing.

I. INTRODUCTION

According to the World Health Organization [1], severe pneumonia is associated with a respiratory rate of more than 30 breaths per min. The respiratory rate is extensively used in the triage, diagnosis, and prognosis of the novel coronavirus infection, and the importance of the noncontact monitoring of respiratory rate data has been noted [2]. The adoption of radar technology is a suitable approach for monitoring respiratory diseases because microwaves and millimeter-waves can

The associate editor coordinating the review of this manuscript and approving it for publication was Brian Ng¹.

penetrate clothes, bedding, and similar fabric obstacles, allowing radar systems to measure skin displacements generated by the physiological signals of distant people accurately, without requiring sensors. In this study, we developed a noncontact measurement system for respiration monitoring using a millimeter-wave array radar system based on a novel clustering algorithm that exploits individual respiratory differences, with the aim of monitoring the respiration of several people simultaneously and with high accuracy. The proposed method implements a series of processes, including the automatic detection of people, estimation of the number and locations of people, signal separation, and

respiratory measurement. We thereby demonstrate accurate and noncontact respiratory measurement of several people, which cannot be realized using conventional methods.

Radar-based noncontact respiratory measurements covering multiple human targets have been extensively studied [3]–[21]. However, such conventional studies have targeted only two participants [3]–[12] or a handful of participants [13]–[21]. Most previous studies on the noncontact respiratory measurement of several people assumed ideal conditions; e.g., Yang *et al.* [14] and Su *et al.* [17] assumed a special case where all participants were at different distances from the radar antenna while Xiong *et al.* [13] and Ding *et al.* [15] assumed a special case where all participants were lined up in a straight line. Excluding studies that impose such special conditions, there are no examples of simultaneous noncontact respiratory measurement involving several people to the best of our knowledge.

Some previous studies focused only on the detection of respiration [7], [19], [22] whereas others demonstrated the estimation of the respiration rate. In addition, respiratory rates obtained using a reference respiratory monitor belt and a radar system have been compared [5], [9], [13]–[15]. For example, Lu *et al.* [9] quantitatively evaluated the respiratory-rate estimation accuracy for two participants. However, no study has quantitatively evaluated the accuracy of respiratory rate estimation for several people using radar. In this study, we quantitatively evaluate the accuracy of the estimated respiratory rate of several people.

Furthermore, most previous studies assumed that the number of people to be measured is known in advance. However, to apply such methods in a real environment, it is necessary to find a technique for estimating the number of people. Besides respiratory measurement studies, methods for estimating the number of people were proposed by Choi *et al.* [23] and Yavari *et al.* [24]. However, as these methods include neither target location estimation nor respiratory measurement, they are unsuitable for the purpose of this study. A method for estimating the number of people by detecting their respiration was proposed by Lv *et al.* [22], and methods for estimating the number and locations of people by detecting their respiration were proposed by Ha *et al.* [7] and Novák *et al.* [19]; however, these methods were not designed for the measurement of the respiratory rate.

In this study, we develop a radar-based system for noncontact respiratory measurement involving several people, when the number and locations of people are unknown. More specifically, to separate multiple radar echoes, instead of the traditional approach involving the application of clustering in the real space, the proposed method applies clustering to high-dimensional space constructed by converting the estimated respiratory intervals into virtual distances used with real-space variables. Hereafter, we refer to this multidimensional space as the respiratory-space. Clustering in the respiratory-space allows for the clear separation and discrimination of multiple radar echoes from targets in proximity, and the accurate measurement of the respiration rates

of several people simultaneously, even under crowded conditions. We performed radar measurement experiments with up to seven participants, and quantitatively evaluated the performance of the proposed method by comparing the results with reference data obtained from belt-type respirometer sensors worn on the chests of the participants. The experimental results demonstrate that our proposed respiratory-space clustering outperforms the conventional real-space clustering approach, realizing accurate and simultaneous measurement of the respiration of several people.

Regarding the selection of the operating frequency, low-frequency microwaves (e.g., microwaves having a frequency of 2.4 GHz) have been used [6]–[8], [13], [15] because devices operating at these frequencies are inexpensive and the microwaves penetrate clothing well. Radar at higher frequencies is also used because it is sensitive to small body displacements; for example, Islam *et al.* [5], Muragaki *et al.* [4], and Walterscheid *et al.* [16] respectively used 24-, 60-, and 72-GHz radar systems for respiratory measurement. In the present study, we used a 79-GHz radar system that is suitable for detecting small body movement generated by respiration. As for the bandwidth, existing studies reported radar-based respiratory measurements made using signals with various bandwidths, such as 0.4 GHz [3], 1.0 GHz [16], [17], 1.3 GHz [4], 1.5 GHz [7], 2.5 GHz [14], 3.0 GHz [6], 3.3 GHz [18], 4.5 GHz [19], and 8.7 GHz [15]. To separate echoes from multiple people effectively, we used a radar system that had a bandwidth of 3.5 GHz in this study.

II. RESPIRATORY MEASUREMENT FOR MULTIPLE PEOPLE USING AN ARRAY RADAR

A. MILLIMETER-WAVE ARRAY RADAR

In this study, we used a millimeter-wave multiple-input and multiple-output (MIMO) array radar system to measure the respiration of multiple people. The proposed system estimates the number and locations of the target people using the received signals and then outputs the respiratory movements and respiratory rate of each person. Figure 1 presents a photograph of the radar system used in this study.



FIGURE 1. Photograph of the radar system developed and used in this study.

This study adopted a frequency-modulated continuous-wave (FMCW) radar system with a center frequency of 79 GHz, center wavelength $\lambda = 3.8$ mm, and a range resolution of 43 mm. The transmission power was 9 dBm, and the equivalent isotropic radiation power was 20 dBm. The system had an MIMO antenna array with three elements for transmission and four elements for reception, allowing a total of 12 signal channels to be acquired. The transmitting and receiving elements were arranged in equally spaced linear arrays at intervals of 2λ (7.6 mm) and $\lambda/2$ (1.9 mm), respectively. In general, MIMO arrays can be approximated by virtual arrays in cases where the distance between the target and antennas is sufficiently larger than the array aperture length, and the mutual coupling between the elements is negligible. The array of the above radar system can be approximated by a 12-element linear virtual array with half-wavelength spacing. The element patterns of each element were $\pm 4^\circ$ and $\pm 35^\circ$ on the E- and H-planes, respectively. The three transmitting elements repeated transmission with time-division multiplexing, and a total of 12 channels of the signal were stored every 100 ms, resulting in a slow-time sampling frequency of 10 Hz that is sufficiently high for respiratory measurement but too low for the measurement of the heartbeat.

Figure 2 is a diagram of the chirp signal transmission of the radar system used in time-division multiplexing that is applied only to the transmitters and not to the receivers. The chirp duration was 267 μ s, the interval between consecutive chirps was 57 μ s, and the three transmitting elements thus transmitted signals sequentially with intervals of 324 μ s. After transmitting all 48 chirps, there was a blank time. Note that the time difference between the first and third transmitting signals was 648 μ s, which was sufficiently small for a typical Doppler shift generated by respiration at 79 GHz. We therefore regard the radar signals for the three transmitting elements to be coherent hereafter. Note also that the range resolution (43 mm) of the radar system was not identical to the minimum distance between two people in the line-of-sight direction that could be distinguished by the radar. We confirmed through measurements that the minimum separation distance was around 180 mm, which is more than four times the range resolution.

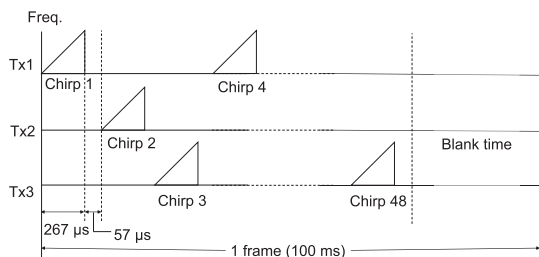


FIGURE 2. Chirp signal transmission diagram of the radar system in this study.

B. RADAR IMAGING OF MULTIPLE PEOPLE

Figure 3 presents an overview of the entire system. The signal received by the FMCW radar can be converted into

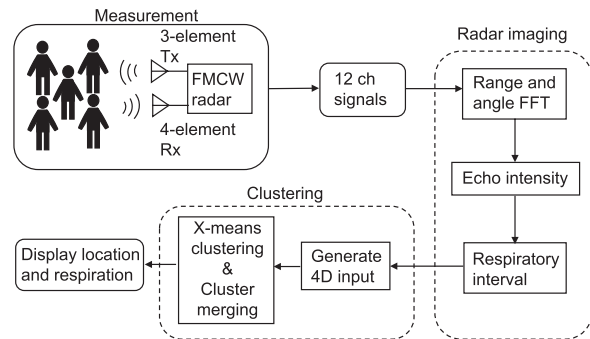


FIGURE 3. Overview of the radar-based respiratory measurement system for multiple human targets.

range-domain data by applying a Fourier transform in the fast-time direction, and it is expressed as $s_k(t, r)$ ($k = 0, 1, \dots, K - 1$). Here, $K = 12$ is the number of elements in the virtual array, and variables t and r represent the slow time and range, respectively. The x coordinate of the k -th virtual array element is denoted $x_k = k\lambda/2$. Each received signal is multiplied by the calibration correction factor c_k and the Taylor window coefficient τ_k to obtain the signal vector $s(t, r)$, which is defined by

$$s(t, r) = [\tau_0 c_0 s_0(t, r), \tau_1 c_1 s_1(t, r), \dots, \tau_{K-1} c_{K-1} s_{K-1}(t, r)]^T, \quad (1)$$

where the superscript T denotes the transpose of the matrix. The beamforming technique is applied to this signal vector to obtain a complex radar image $I_0(t, r, \theta) = \mathbf{w}^H(t, r) s(t, r)$. Here, the superscript H represents the complex conjugate transposition of the matrix, and the beamforming weight coefficient vector $\mathbf{w}(\theta) = [w_0, w_1, \dots, w_{K-1}]^T$, with $w_k(\theta) = e^{-j(2\pi x_k/\lambda) \sin \theta} = e^{-j\pi k \sin \theta}$ ($k = 0, 1, \dots, K - 1$).

When calculating $I_0(t, r, \theta)$, we discretize θ into unequal intervals $\theta_0, \theta_1, \dots, \theta_{N-1}$. By selecting θ_n such that $\sin \theta_n = n/N$ ($n = 0, 1, \dots, N - 1$), we obtain $w_k(\theta_n) = e^{-j\pi kn/N}$. By selecting $N = K$, the equation becomes equivalent to a discrete Fourier transform in the element number direction, allowing the fast Fourier transform algorithm to be used for implementation.

The complex radar image $I_0(t, r, \theta)$ contains static clutter, which is the unwanted response from the stationary objects, in addition to the echoes from the human targets. To remove the static clutter, we subtract the DC component (i.e., the time average) to obtain the complex radar image $I_c(t, r, \theta)$ in which the static clutter is suppressed:

$$I_c(t, r, \theta) = I_0(t, r, \theta) - \frac{1}{T_c} \int_{t-T_c}^t I_0(\tau, r, \theta) d\tau. \quad (2)$$

Furthermore, the power of the complex radar image is time-averaged to obtain the radar image $I_P(t, r, \theta)$:

$$I_P(t, r, \theta) = \frac{1}{T_P} \int_{t-T_P}^t |I_c(\tau, r, \theta)|^2 d\tau, \quad (3)$$

where T_c and T_P are set to 30 and 20 s, respectively.

In most previous studies in this field, $I_p(t, r, \theta)$ has been used to detect multiple human targets and estimate their locations. The typical approach involves the application of a clustering algorithm in the real space represented by (r, θ) . In this paper, we propose a novel approach in which estimated respiration rate values are exploited to discriminate echoes from human bodies, where the respiration rate is estimated even before estimating the number and locations of the human targets, as described in the next section. This step is the core idea of our proposed system for accurately discriminating the radar echoes from human targets in proximity.

Note that the DC suppression process in Eq. (2) can cause waveform distortion, which may lower the accuracy of the proposed method. The effect of the DC offset on the physiological measurement has been intensively studied [25], [26] and will be considered in our future work.

C. RESPIRATORY IMAGING OF MULTIPLE PEOPLE

In most previous studies, the location (r_0, θ_0) of each target person is first determined, after which vital signs such as the respiration are extracted from the signal $I_c(t, r_0, \theta_0)$ corresponding to the location. In our proposed approach, we attempt to estimate the respiratory interval at all the locations (r, θ) without specifying the location of the human target. As a result, the respiratory interval can be expressed as a function of t, r , and θ . In this paper, this image is referred to as the respiratory image.

We first estimate the displacement waveform of the target from the phase variation of the reflected waves as

$$d_0(t, r, \theta) = \frac{\lambda}{4\pi} \angle I_c(t, r, \theta). \quad (4)$$

We next apply a bandpass filter to $d_0(t, r, \theta)$ and obtain $d(t, r, \theta)$, where the cut-off frequencies of the filter correspond to 11 and 51 s. This bandpass filter suppresses the low-frequency component, which mainly contains body movement, and the high-frequency component, which mainly contains noise.

Finally, the respiratory interval at time t is determined as a function of r and θ as $\tau_r(t, r, \theta)$ by solving an optimization problem:

$$\tau_r(t, r, \theta) = \arg \min_{0 < \tau \leq T_0} f_{t,r,\theta}(\tau), \quad (5)$$

where we set $T_0 = 8.0$ s, and the cost function $f_{t,r,\theta}(\tau)$ is expressed as

$$f_{t,r,\theta}(\tau) = \frac{1}{2T_0} \int_{t-2T_0}^t |d(t', r, \theta) - d(t' + \tau, r, \theta)|^2 + |d(t', r, \theta) - d(t' - \tau, r, \theta)|^2 dt'. \quad (6)$$

The resultant image $\tau_r(t, r, \theta)$ is called respiratory image that is used in our proposed clustering method. In the implementation of the above algorithm, $\tau_r(t, r, \theta)$ does not represent a respiratory interval when there is no echo from a human target at (r, θ) . The computational load can be reduced by setting a certain threshold and calculating the respiratory

image $\tau_r(t, r, \theta)$ only for (t, r, θ) with the radar image exceeding the threshold.

III. ESTIMATION OF THE NUMBER AND LOCATIONS OF MULTIPLE HUMAN TARGETS WITH CLUSTERING

A. CONVENTIONAL X-MEANS CLUSTERING WITH AN UNKNOWN NUMBER OF CLUSTERS

Numerous studies on radar imaging and tracking used clustering algorithms to separate echoes from multiple targets, including human bodies [27]–[41]. In this study, we also adopted the x-means clustering algorithm [42], which is an extension of the well-known k -means algorithm, because the x-means algorithm does not require the number of clusters whereas the k -means algorithm does. The x-means algorithm is therefore suitable for situations where the number of targets is unknown, as in this study. The x-means algorithm includes the following steps [42].

- 1) Let cluster C represent all the input data (the point cloud).
- 2) Process the point cloud $\mathbf{x} \in C$ using the k -means method with $k = 2$ to generate clusters C_1 and C_2 .
- 3) Calculate the Bayesian information criterion for cluster C and for the two segmented models C_1 and C_2 . Let the former criterion be b and the latter be b' .
- 4) If $b \leq b'$, adopt cluster C before the split.
- 5) If $b > b'$, adopt the split clusters C_1 and C_2 and return to step (2), setting $C_1 \rightarrow C$. Then repeat step (2) setting $C_2 \rightarrow C$.

In the conventional approach, the initial point cloud C is generated from the radar image $I_p(t, r, \theta)$ alone, whereas in the next section, we introduce a respiratory-space representation as the point cloud C that contains information on the respiratory characteristics estimated from the complex radar image $I_c(t, r_0, \theta_0)$. At time t , a point cloud is generated in the r - θ domain from the radar image $I_p(t, r, \theta)$ and clustered using the x-means algorithm, where the number of targets is obtained from the estimated number of clusters. The target locations are estimated from the centroid of each cluster. We refer to the clustering method explained in this section as conventional two-dimensional (2D) clustering.

B. PROPOSED RESPIRATORY-SPACE CLUSTERING

In this section, we propose a new clustering method, respiratory-space clustering, to separate the radar echoes of multiple breathing human targets and determine the target number and locations. The proposed method estimates the respiratory interval for each location (r, θ) prior to clustering, increasing the dimensionality of the input point cloud by converting the respiratory intervals into virtual spatial coordinates. The resulting high-dimensional space is called the respiratory space. The point cloud in the respiratory space is then processed using the x-means algorithm to estimate the number and locations of people.

The range r and azimuth θ are discretized and denoted r_l and θ_n ($l = 1, 2, \dots, L$; $n = 1, 2, \dots, N$), respectively. The sampling interval of the range r is a constant value Δr , while

the angles θ are sampled at unequal intervals, as described in Section II-B. In this paper, we define the four-dimensional vector $\mathbf{x}_{l,n}$ in the respiratory space at time t as

$$\mathbf{x}_{l,n} = [r_l, \theta_n, \tau_r(t, r_l, \theta_n), \tau_r(t - T_{cy}, r_l, \theta_n)]^T, \quad (7)$$

where $T_{cy} = 6.0$ s. This four-dimensional vector contains the respiratory intervals calculated at time t and $t - T_{cy}$ in addition to the physical coordinates (r, θ) . To suppress the effects of noise and random components, we use respiratory intervals averaged for time T_{cy} , which is approximately a typical respiratory interval, and apply a median filter sized 3×4 .

When generating the point cloud to be input to the clustering algorithm, it is preferable that the point density is high for (r, θ) having a large value in the radar image I_P . The number of point cloud points $\rho_{l,n} \in \mathbb{Z}$ used for clustering is given by

$$\rho_{l,n} = [\alpha r_l I_P(t, r_l, \theta_n)], \quad (8)$$

where α is a constant, $[\cdot]$ represents the integer closest to the value of the real number, and r_l is a multiplicative factor that compensates for propagation loss. Using this formula, points were generated in four-dimensional space. This process is repeated for all (l, n) to generate the point cloud, which is then passed as input to the x-means algorithm for clustering.

C. PROPOSED CLUSTER MERGING METHOD

In the proposed method, two or more clusters may be generated erroneously for the same target. In such cases, the corresponding clusters would be located close to each other. Such an erroneous clustering can be detected by considering the typical size of the human body D , where we set $D = 0.6$ m empirically. In this paper, we propose the following steps for merging multiple clusters that have been incorrectly split. Let us assume that M clusters C^1, C^2, \dots, C^M are generated using the method proposed in the previous section.

- 1) Calculate the centroid of each cluster. The centroids, denoted by $\mathbf{c}_1, \mathbf{c}_2, \dots, \mathbf{c}_M$, are points on the x - y plane, which are the Cartesian coordinates converted from the r - θ plane.
- 2) Calculate the distance $g_{i,j} = \|\mathbf{c}_i - \mathbf{c}_j\|$ ($i, j = 1, 2, \dots, M$) between each centroid pair.
- 3) If $D > \min_{i,j} g_{i,j}$, merge clusters C^{i^*} and C^{j^*} letting $(i^*, j^*) = \arg \min_{i,j} g_{i,j}$ and return to step (1) unless $D \leq \min_{i,j} g_{i,j}$.

The final number of clusters generated by the above process is output as an estimate of the number of participants. After applying this cluster merging method, the representative position of each cluster is determined as the position where the value of the radar image I_P is a maximum within the cluster area.

IV. PERFORMANCE EVALUATION OF THE PROPOSED RESPIRATORY-SPACE CLUSTERING

A. OVERVIEW OF THE EXPERIMENTAL SETUP

We conducted experiments to evaluate the performance of the proposed respiratory-space clustering method for the

respiratory measurement of multiple human targets. The participants were seated and stationary. Experiment 1 assumed seven seated participants spaced at approximately 1-m intervals (Fig. 4), whereas experiment 2 assumed five seated participants spaced at approximately 0.7-m intervals (Fig. 5). The seven participants in experiment 1 were seated in a U-shaped arrangement, as shown in the right panel of Fig. 4. The four participants in experiment 2 were seated at the corners of a 1-m square, with the fifth participant at the center, as depicted in the right panel of Fig. 5. In both experiments, the coordinates of the center of the radar array were used as the origin. The measurement time was 120 s in both experiments, and the participants were instructed to remain still and breathe naturally during the measurement. We simultaneously measured the respiratory rate using belt-type sensors worn on the chests of the participants to quantitatively evaluate the accuracy of the respiratory rate estimated using the proposed radar-based approach.

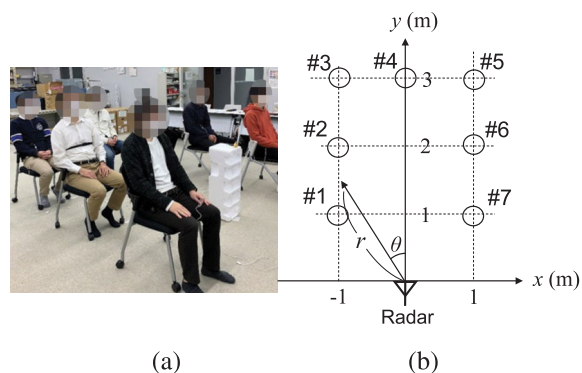


FIGURE 4. Experiment 1: Experimental validation with seven participants (a) and their seating positions (b).

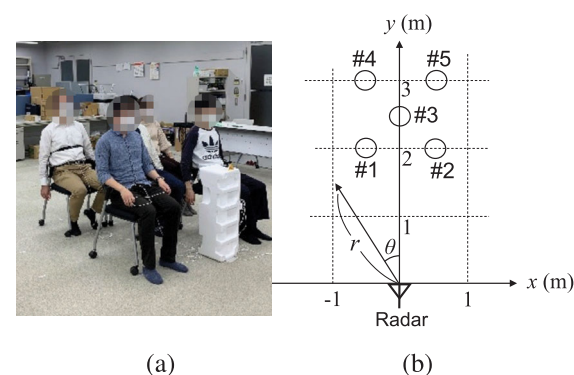


FIGURE 5. Experiment 2: Experimental validation with five participants in proximity (a) and their seating positions (b).

B. EVALUATION OF THE NUMBER AND LOCATION ESTIMATES

1) EXPERIMENT 1

Figure 6 presents an example of the radar image $I_P(t, r, \theta)$ captured in experiment 1 with the seven participants. Note that $I_P(t, r, \theta)$ has been normalized with the noise floor.

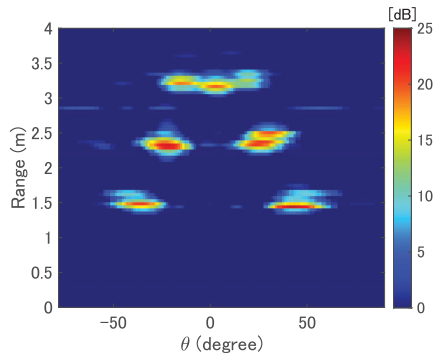


FIGURE 6. Example of the radar image $I_P(t, r, \theta)$ (experiment 1).

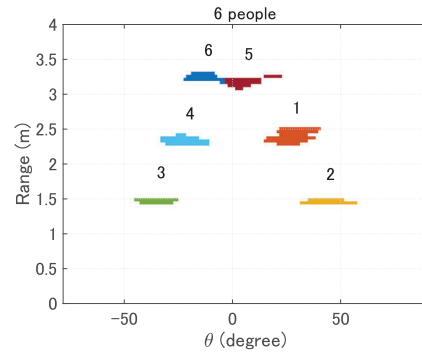


FIGURE 8. Estimation using conventional 2D clustering (experiment 1).

In this figure, strong responses are seen at the approximate seating positions of the seven participants. Figure 7 shows an example of the respiratory image $\tau_r(t, r, \theta)$, where different respiratory intervals are observed at the seating positions.

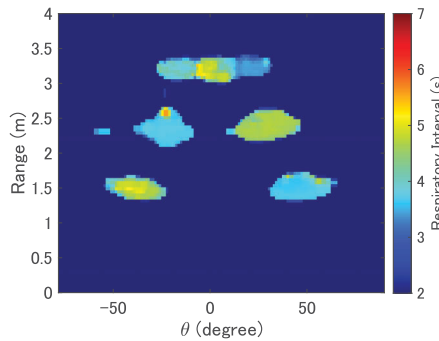


FIGURE 7. Example of the respiratory image $\tau_r(t, r, \theta)$ (experiment 1).

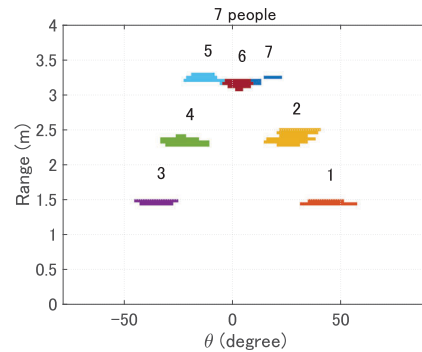


FIGURE 9. Estimation using the proposed respiratory space clustering (experiment 1).

We next present the clusters obtained using the conventional and proposed clustering methods. We applied conventional clustering in 2D space (r, θ) and the proposed clustering in four-dimensional (4D) space ($r, \theta, \tau_1, \tau_2$). Figure 8 shows the clusters obtained using the conventional 2D clustering. Note that the cluster numbers do not necessarily match the participant numbers shown in Fig. 4. Although four participants within a range of 2.5 m were correctly clustered, three participants at ranges greater than 3 m were incorrectly clustered into two clusters; i.e., the number of people was estimated incorrectly. When the targets are located far from the radar antennas, multiple targets in the $r-\theta$ space become closer in the angle direction, making them more difficult to separate.

Figure 9 shows the clusters generated using the proposed 4D respiratory-space clustering for the same time instance as in Fig. 8; all the participants are correctly clustered regardless of the range. Because the x-means algorithm is initialized with random numbers, the estimated number of targets depends on the random numbers. To evaluate the accuracy in estimating the number of targets, we ran the algorithm with 100 random seeds. Because the proposed method performed clustering 11 times over a measurement duration

of 120 s, the total number of clustering trials was 1100 for 100 seeds. Among the 1100 clustering trials, the number of targets was correctly estimated 100 and 1073 times using the conventional 2D clustering and the proposed 4D clustering, respectively. These numbers correspond to 9.1% and 97.6% of accuracies in the estimation of the number of targets. Thus, high-dimensional clustering, which incorporates the respiratory intervals in the input vector, is an effective approach for accurately estimating the number of human targets.

Finally, we present the locations of the participants estimated using the proposed method. The participant locations estimated using the proposed respiratory-space clustering technique are depicted in Fig. 10. Note that Fig. 10 shows the locations averaged over the measurement time, where the participant numbers match the numbering shown in Fig. 4. The estimated coordinates of the seven participants appear to be correct, and they approximately match the image on the right of Fig. 4. However, as the actual participant locations cannot be determined precisely and it is difficult to determine the part of the body contributing to the echo reflection because of the complex shape of the human body, it was not possible to evaluate the accuracy of the estimated locations.

2) EXPERIMENT 2

Figures 11 and 12 show examples of the radar image $I_P(t, r, \theta)$ and respiratory image $\tau_r(t, r, \theta)$ in experiment 2 with five participants. Participants 1 and 2 had similar

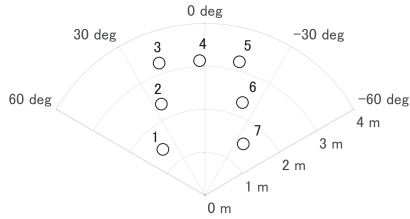


FIGURE 10. Subject locations estimated using the proposed respiratory-space clustering technique (experiment 1).

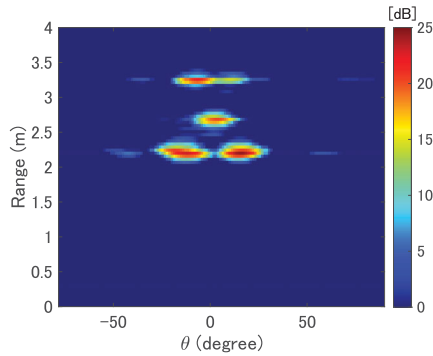


FIGURE 11. Example of the radar image $I_p(t, r, \theta)$ (experiment 2).

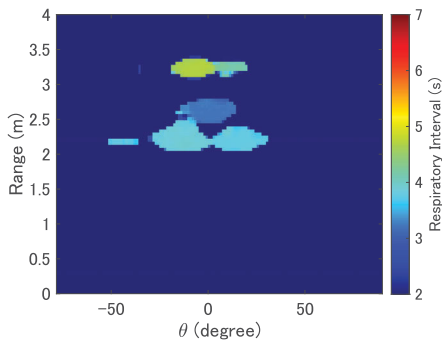


FIGURE 12. Example of the respiratory image $\tau_r(t, r, \theta)$ (experiment 2).

respiratory intervals by coincidence, whereas the other three participants had different respiratory intervals.

As for experiment 2, we compare the results of conventional 2D clustering with those of the proposed respiratory-space clustering. Figure 13 shows the clusters estimated using conventional 2D clustering. Three participants within a range of 3 m from the radar were separated correctly, but the two participants located at a range of approximately 3.5 m were incorrectly grouped into one cluster. As in experiment 1, distant participants were more difficult to segregate in the angular direction.

Figure 14 presents the clusters obtained using the proposed respiratory-space clustering at the same time instance as in Fig. 13. The proposed method correctly separates the two participants at a range of approximately 3.5 m and accurately estimates the number of people. As mentioned above, clustering was performed 11 times in total during the measurement time. Among the 1100 clustering trials for 100 seeds, the number of targets was correctly estimated 200

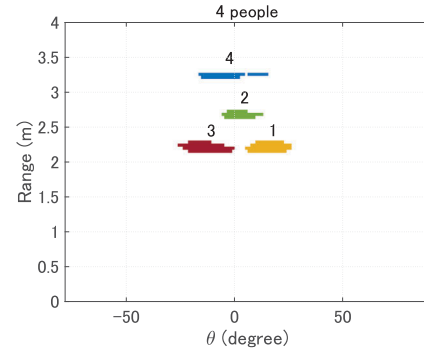


FIGURE 13. Clusters estimated using conventional 2D clustering (experiment 2).

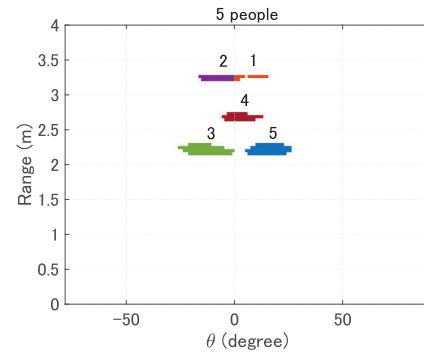


FIGURE 14. Clusters estimated using the proposed respiratory-space clustering (experiment 2).

and 1096 times using the conventional 2D clustering and the proposed 4D clustering, respectively. These numbers correspond to 18.2% and 99.6% of accuracies in the estimation of the number of targets. Thus, as in experiment 1, it was demonstrated that high-dimensional clustering is effective in estimating the accurate number of target people. Finally, we present the estimated locations of the human targets. The target locations estimated using the respiratory-space clustering technique are shown in Fig. 15; the five participants approximately match the image on the right of Fig. 5.

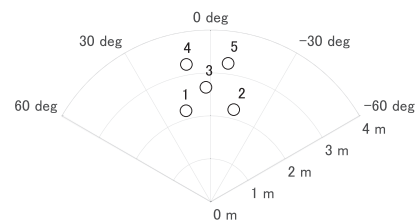


FIGURE 15. Participant locations estimated using the proposed respiratory-space clustering technique (experiment 2).

C. PERFORMANCE EVALUATION OF THE PROPOSED METHOD FOR DIFFERENT LAYOUTS OF PEOPLE

To investigate the performance of the proposed method for other layouts of the participants, we conducted five additional measurements with different layouts, which are referred to as experiments 3, 4, 5, 6, and 7. Figures. 16-20 show the

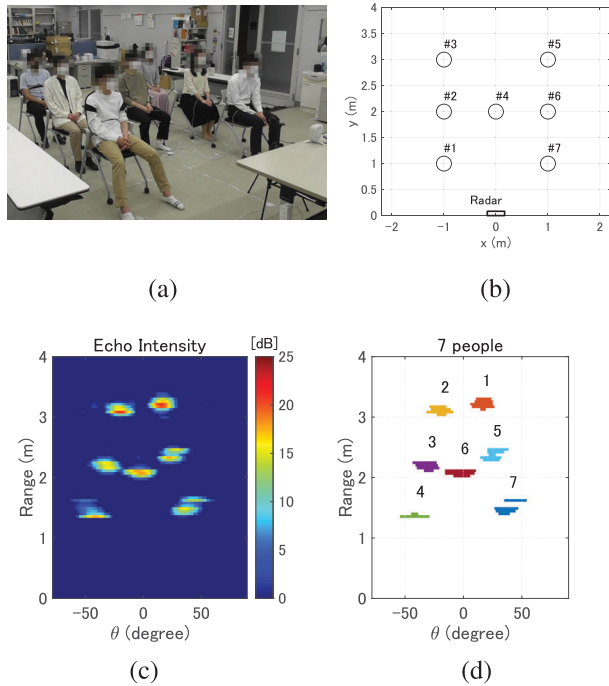


FIGURE 16. Experiment 3 with seven participants (a), their seating positions (b), the radar image (c), and clusters estimated using the proposed respiratory-space clustering (d).

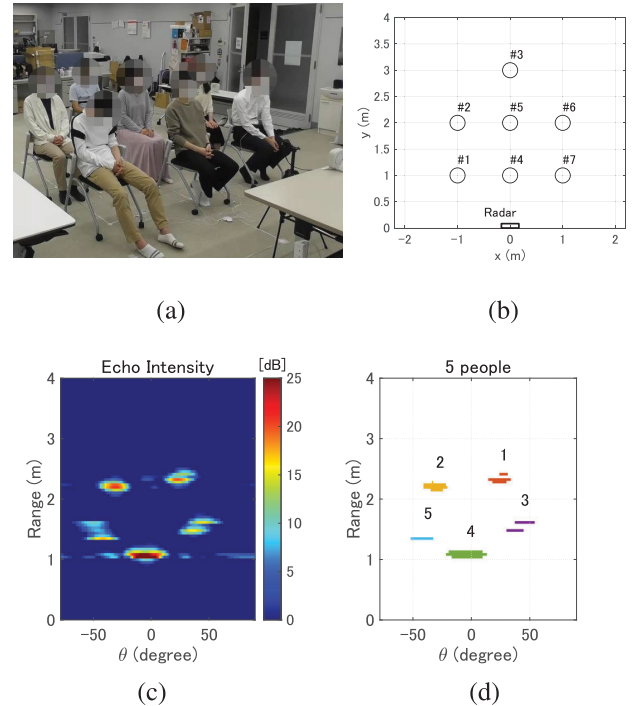


FIGURE 18. Experiment 5 with seven participants (a), their seating positions (b), the radar image (c), and clusters estimated using the proposed respiratory-space clustering (d).

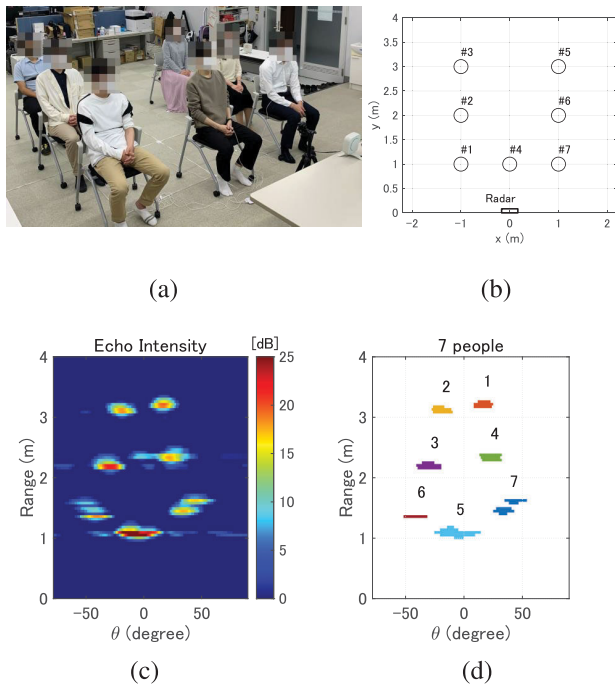


FIGURE 17. Experiment 4 with seven participants (a), their seating positions (b), the radar image (c), and clusters estimated using the proposed respiratory-space clustering (d).

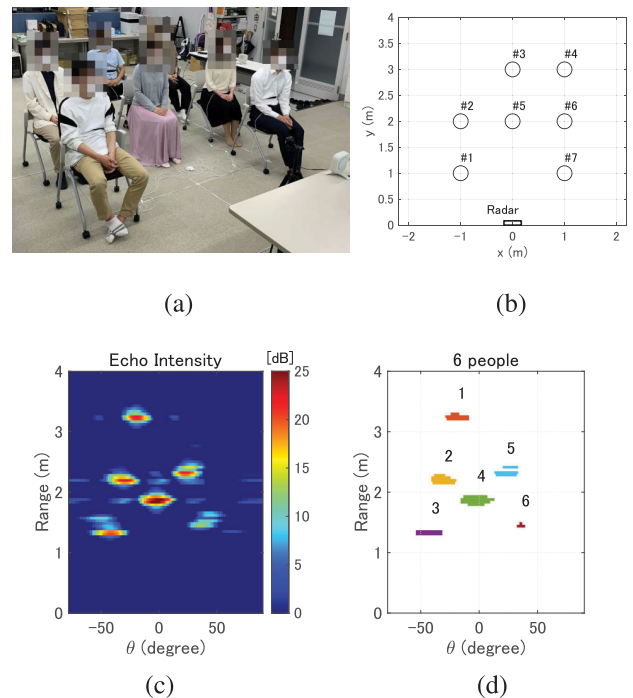


FIGURE 19. Experiment 6 with seven participants (a), their seating positions (b), the radar image (c), and clusters estimated using the proposed respiratory-space clustering (d).

photograph of the measurement scenario in (a), the actual layout of participants in (b), the radar image in (c), and the clusters obtained using the proposed method (d) for each experiment. In these experiments, seven participants were

instructed to breathe normally as in experiments 1 and 2. As seen in the figures, the number of people was estimated to be 7, 7, 5, 6, and 5 in experiments 3, 4, 5, 6, and 7, respectively. The number was correctly estimated in experiments 3 and 4,

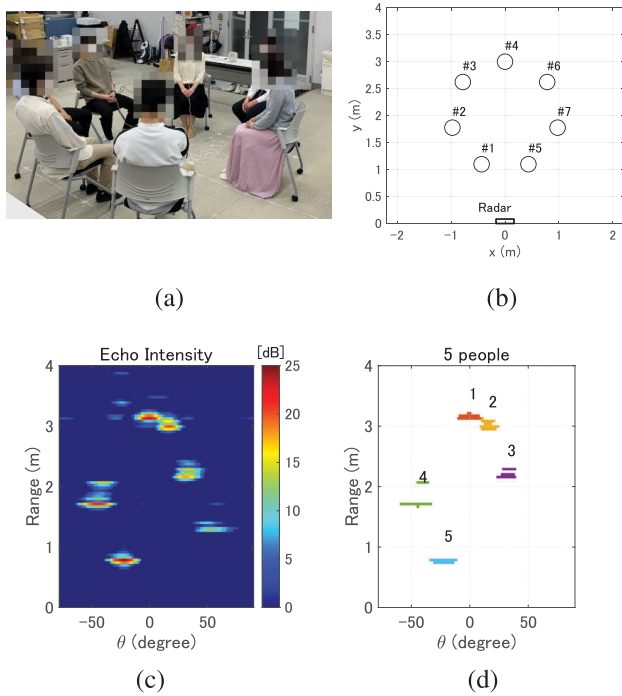


FIGURE 20. Experiment 7 with seven participants (a), their seating positions (b), the radar image (c), and clusters estimated using the proposed respiratory-space clustering (d).

whereas the echoes from a few people were not detected in experiments 5, 6, and 7. These results are explained by shadowing; an echo from a person is blocked by the body of another person. Despite this limitation due to shadowing, the proposed method was demonstrated to be able to measure the physiological signals of multiple people.

D. EVALUATION OF THE RESPIRATORY INTERVAL ESTIMATION ACCURACY

A commonly used indicator of the respiratory status is the respiratory rate, which is the number of breaths per minute and proportional to the reciprocal of the respiratory interval. We evaluated the accuracy of the proposed method in terms of instantaneous respiratory intervals that are not averaged over a period of 1 minute. We applied our proposed method to the radar signal in estimating the respiratory intervals, and evaluated the accuracy of the estimated respiratory intervals by comparing them with the values obtained using belt-type contact respirometers, which are assumed to be the true values.

Figure 21 and 22 present normalized displacements of the participants that are obtained using the radar system and respirometers in experiments 1 and 2. Note that the figures show the displacements only for 30 s that are extracted from the total measurement time. Table 1 gives the actual number of participants M_{tr} and the number of participants estimated using the proposed method M_{est} for the seven experiments. In addition, Table 1 summarizes the root-mean-square error (RMSE) in estimating the respiratory

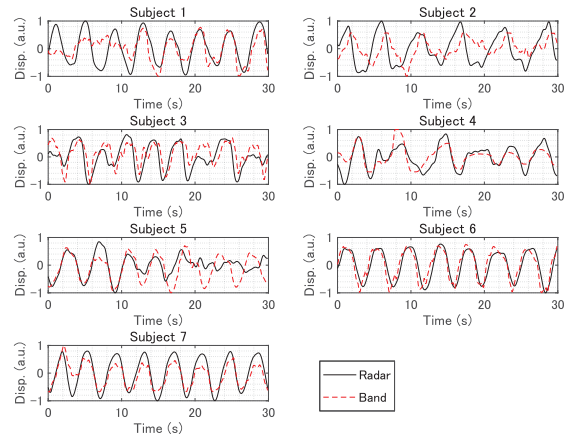


FIGURE 21. Normalized displacements of participants obtained using a radar system and belt-type contact respirometers (experiment 1).

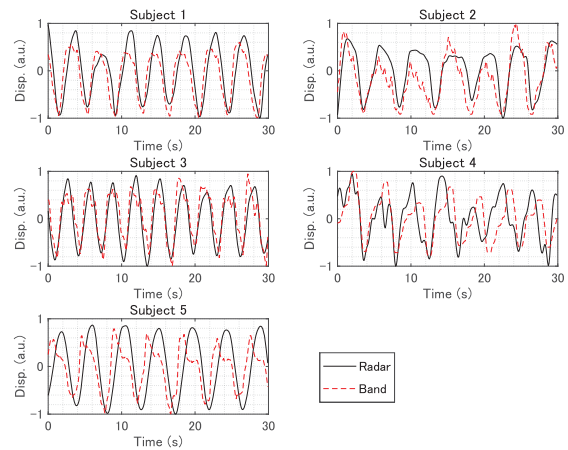


FIGURE 22. Normalized displacements of participants obtained using a radar system and belt-type contact respirometers (experiment 2).

TABLE 1. Root-mean-square error in estimating the respiratory interval of each participant using the proposed method.

Exp. No.	M_{tr}	M_{est}	RMSE for each participant (ms)						
			1	2	3	4	5	6	7
1	7	7	121	112	51	541	306	34	428
2	5	5	54	134	66	154	66	-	-
3	7	7	168	141	115	169	73	226	226
4	7	7	401	217	168	118	51	227	321
5	7	5	268	131	-	141	-	144	115
6	7	6	154	113	-	90	118	182	270
7	7	5	-	124	197	453	799	-	240

intervals using the proposed method for each participant. Note that the RMSE is not presented in the table when the participant was not detected. The average RMSE for all participants in the seven experiments was 196 ms, which is sufficiently smaller than a typical respiratory interval (e.g., 3–5 s), demonstrating that our system can estimate the respiratory interval with high accuracy. The results also indicate that the proposed method can estimate the respiratory intervals of the detected people accurately even when the number of people is incorrectly estimated.

E. PERFORMANCE EVALUATION OF THE PROPOSED METHOD FOR DIFFERENT RADAR POSITIONS

We investigate the effect of the radar position on the performance of the proposed method by analyzing two additional datasets with a radar system located at different positions (x_2, y_2) (position 2) and (x_3, y_3) (position 3), where $x_2 = 2$ m, $y_2 = 2$ m, $x_3 = -2$ m, and $y_3 = 2$ m. The layout of the participants is the same as that in experiment 1 (Fig. 4). Figure 23 shows the radar images in (a) and (c) and the clusters estimated using the proposed method in (b) and (d). Panels (a) and (b) are obtained with the radar system in position 2 whereas panels (c) and (d) are obtained with the radar system in position 3. When the radar was placed in position 3, all seven participants were correctly detected, whereas one of the participants was not detected when the radar was placed in position 2. This result can be explained by the shadowing as mentioned in Section IV-C. The body of a person who is located between the radar system and another person can block the echo, resulting in a missing cluster in the cluster image. This result indicates that although the proposed method works regardless of the radar position, the echo shadowing can prevent an echo from being detected.

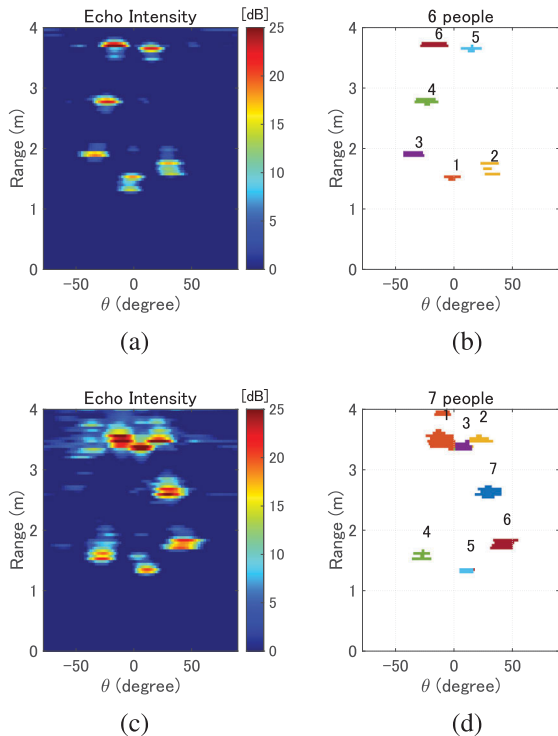


FIGURE 23. Radar images obtained using the radar system located at position 2 (a) and position 3 (c) and clusters estimated using the proposed method and radar system located at position 2 (b) and position 3 (d).

F. PERFORMANCE OF THE PROPOSED METHOD FOR NON-STATIC PEOPLE

So far, we have assumed a relatively static situation where the participants were instructed to remain still while breathing normally. In this subsection, we evaluate the performance of

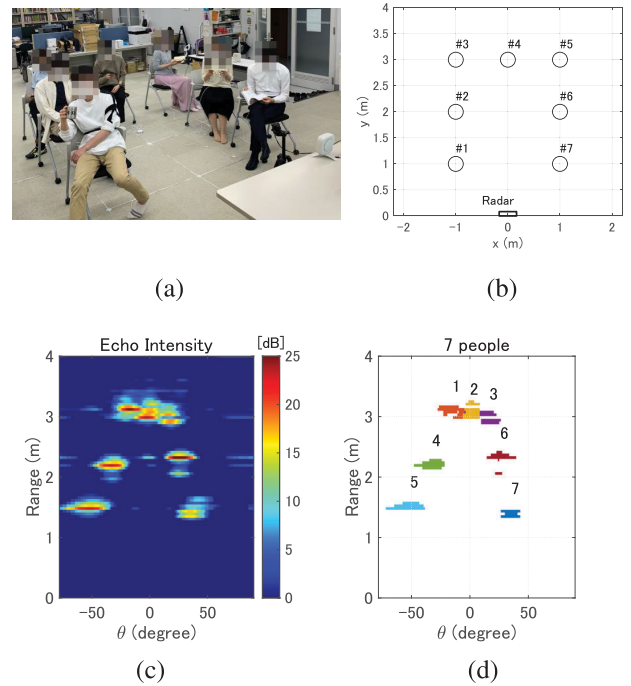


FIGURE 24. Experimental validation in a non-static situation where the participants perform small movements, such as the situations of holding a smartphone or reading a book (a), their actual positions (b), the radar image (c), and clusters estimated using the proposed respiratory-space clustering (d).

the proposed method when the participants were instructed to behave normally while drinking coffee, reading a book, and handling a smartphone. Panels (a) and (b) in Fig. 24 respectively show the photograph of the measurement scenario and the actual layout of participants. Note that the layout of the participants is the same as that in experiment 1. Panels (c) and (d) in Fig. 24 respectively show a radar image and the estimated clusters. As seen in Fig. 24, all seven participants were correctly separated and detected even in the non-static situation. This result indicates the possible applicability of the proposed method to a realistic scenario. Additional study is necessary to investigate the performance of the proposed method in realistic situations so that the proposed method can be extended to perform well in practical settings; this is left as future work.

In this paper, we assumed that the radar measurements were made under a condition with little to no multipath propagation. In real life situations, however, the effect of multipath propagation must be taken into account. Some studies reported radar-based physiological measurement techniques that work even in a multipath-rich environment [43]–[46]. It is important to improve the accuracy of the proposed method when it is applied to measurement data recorded in a multipath-rich environment.

V. CONCLUSION

In this study, we developed a noncontact respiration monitoring system that simultaneously measures the respiration of several people, even when the number and

locations of people are unknown. To evaluate the proposed respiration monitoring system, we measured the respiration of multiple human targets in eight experiments involving five or seven participants. The obtained results demonstrated that the use of the proposed clustering method in the 4D respiratory space was able to separate echoes accurately and estimate the number and locations of the participants unless some echoes were blocked through shadowing. Using the proposed clustering method instead of the conventional clustering method, the accuracy in estimating the number of people was improved by 88.5% and 81.4% in experiments 1 and 2, respectively, indicating that the proposed method is effective in estimating the number of participants. Belt-type respirometers were used in the experiments to evaluate the accuracy of the respiratory intervals estimated using the radar system and the proposed method. In the experiments, the proposed method had an average RMSE of 196 ms, which is sufficiently smaller than a typical respiratory interval (e.g., 3-5 s). The obtained results demonstrate that the clustering method and system proposed in this study are effective for measuring the respiration of several people accurately and simultaneously even when the number and locations of the people are unknown.

ACKNOWLEDGMENT

A preprint of this manuscript has been posted on arXiv (arXiv:2101.12422 [eess.SP]).

ETHICS DECLARATIONS

This study was approved by the Ethics Committee of the Graduate School of Engineering, Kyoto University, under Approval Nos 201916. Informed consent was obtained from all participants in the study.

REFERENCES

- [1] *Clinical Management of Severe Acute Respiratory Infection When Novel Coronavirus (2019-nCoV) Infection is Suspected: Interim Guidance*, WHO/nCoV/Clin., World Health Org., Geneva, Switzerland, 2020.
- [2] C. Massaroni, A. Nicoló, E. Schena, and M. Sacchetti, "Remote respiratory monitoring in the time of COVID-19," *Frontiers Physiol.*, vol. 11, p. 635, May 2020, doi: [10.3389/fphys.2020.00635](https://doi.org/10.3389/fphys.2020.00635).
- [3] Y. Li, X. Jing, H. Lv, and J. Wang, "Analysis of characteristics of two close stationary human targets detected by impulse radio UWB radar," *Prog. Electromagn. Res.*, vol. 126, pp. 429–447, Mar. 2012.
- [4] M. Muragaki, S. Okumura, K. Maehara, T. Sakamoto, M. Yoshioka, K. Inoue, T. Fukuda, H. Sakai, and T. Sato, "Noncontact respiration monitoring of multiple closely positioned patients using ultra-wideband array radar with adaptive beamforming technique," in *Proc. IEEE Int. Conf. Acoust., Speech Signal Process. (ICASSP)*, New Orleans, LA, USA, Mar. 2017, pp. 1118–1122, doi: [10.1109/ICASSP.2017.7952330](https://doi.org/10.1109/ICASSP.2017.7952330).
- [5] S. M. M. Islam, O. Boric-Lubecke, and V. M. Lubecke, "Concurrent respiration monitoring of multiple subjects by phase-comparison monopulse radar using independent component analysis (ICA) with JADE algorithm and direction of arrival (DOA)," *IEEE Access*, vol. 8, pp. 73558–73569, Apr. 2020, doi: [10.1109/ACCESS.2020.2988038](https://doi.org/10.1109/ACCESS.2020.2988038).
- [6] Y. Wang, Q. Liu, and A. E. Fathy, "Simultaneous localization and respiration detection of multiple people using low cost UWB biometric pulse Doppler radar sensor," in *IEEE MTT-S Int. Microw. Symp. Dig.*, Montreal, QC, Canada, Jun. 2012, pp. 1–3, doi: [10.1109/MWSYM.2012.6258423](https://doi.org/10.1109/MWSYM.2012.6258423).
- [7] T. Ha and J. Kim, "Detection and localization of multiple human targets based on respiration measured by IR-UWB radars," in *Proc. IEEE SENSORS*, Montreal, QC, Canada, Oct. 2019, pp. 1–4, doi: [10.1109/SENSORS43011.2019.8956687](https://doi.org/10.1109/SENSORS43011.2019.8956687).
- [8] O. Boric-Lubecke, V. M. Lubecke, A. Høst-Madsen, D. Samardzija, and K. Cheung, "Doppler radar sensing of multiple subjects in single and multiple antenna systems," in *Proc. 7th, Int. Conf. Telecommun. Mod. Satell., Cable Broadcast. Services (TELSIKS)*, Nis, Serbia, vol. 1, 2005, pp. 7–11, doi: [10.1109/TELSIKS.2005.1572052](https://doi.org/10.1109/TELSIKS.2005.1572052).
- [9] C. Lu, Y. Yuan, C.-H. Tseng, and C.-T. M. Wu, "Multi-target continuous-wave vital sign radar using 24 GHz metamaterial leaky wave antennas," in *IEEE MTT-S Int. Microw. Symp. Dig.*, Nanjing, China, May 2019, pp. 1–4, doi: [10.1109/IMBIOC.2019.8777736](https://doi.org/10.1109/IMBIOC.2019.8777736).
- [10] Q. Wu, Z. Mei, Z. Lai, D. Li, and D. Zhao, "A non-contact vital signs detection in a multi-channel 77 GHz LFM CW radar system," *IEEE Access*, vol. 9, pp. 49614–49628, Mar. 2021.
- [11] X. Shang, J. Liu, and J. Li, "Multiple object localization and vital sign monitoring using IR-UWB MIMO radar," *IEEE Trans. Aerosp. Electron. Syst.*, vol. 56, no. 6, pp. 4437–4450, Dec. 2020.
- [12] M. Nosrati, S. Shahsavari, S. Lee, H. Wang, and N. Tavassolian, "A concurrent dual-beam phased-array Doppler radar using MIMO beamforming techniques for short-range vital-signs monitoring," *IEEE Trans. Antennas Propag.*, vol. 67, no. 4, pp. 2390–2404, Apr. 2019.
- [13] J. Xiong, H. Hong, H. Zhang, N. Wang, H. Chu, and X. Zhu, "Multitarget respiration detection with adaptive digital beamforming technique based on SIMO radar," *IEEE Trans. Microw. Theory Techn.*, vol. 68, no. 11, pp. 4814–4824, Nov. 2020, doi: [10.1109/TMTT.2020.3020082](https://doi.org/10.1109/TMTT.2020.3020082).
- [14] Y. Yang, J. Cao, X. Liu, and X. Liu, "Multi-breath: Separate respiration monitoring for multiple persons with UWB radar," in *Proc. IEEE 43rd Annu. Comput. Softw. Appl. Conf. (COMPSAC)*, Milwaukee, WI, USA, Jul. 2019, pp. 840–849, doi: [10.1109/COMPSAC.2019.00124](https://doi.org/10.1109/COMPSAC.2019.00124).
- [15] C. Ding, J. Yan, L. Zhang, H. Zhao, H. Hong, and X. Zhu, "Noncontact multiple targets vital sign detection based on VMD algorithm," in *Proc. IEEE Radar Conf. (RadarConf)*, Seattle, WA, USA, May 2017, pp. 0727–0730, doi: [10.1109/RADAR.2017.7944298](https://doi.org/10.1109/RADAR.2017.7944298).
- [16] I. Walterscheid, O. Biallawons, and P. Berens, "Contactless respiration and heartbeat monitoring of multiple people using a 2-D imaging radar," in *Proc. 41st Annu. Int. Conf. IEEE Eng. Med. Biol. Soc. (EMBC)*, Berlin, Germany, Jul. 2019, pp. 3720–3725, doi: [10.1109/EMBC.2019.8856974](https://doi.org/10.1109/EMBC.2019.8856974).
- [17] W. C. Su, M. C. Tang, R. El Arif, T. S. Horng, and F.-K. Wang, "Stepped-frequency continuous-wave radar with self-injection-locking technology for monitoring multiple human vital signs," *IEEE Trans. Microw. Theory Techn.*, vol. 67, no. 12, pp. 5396–5405, Dec. 2019, doi: [10.1109/TMTT.2019.2933199](https://doi.org/10.1109/TMTT.2019.2933199).
- [18] N. V. Rivera, S. Venkatesh, C. Anderson, and R. M. Buehrer, "Multi-target estimation of heart and respiration rates using ultra wideband sensors," in *Proc. 14th Eur. Signal Process. Conf.*, Florence, Italy, 2006, pp. 1–6.
- [19] D. Novak and D. Kocur, "Multiple static person localization based on respiratory motion detection by UWB radar," in *Proc. 26th Int. Conf. Radioelektronika*, Kosice, Slovakia, Apr. 2016, pp. 252–257, doi: [10.1109/RADIOELEK.2016.7477386](https://doi.org/10.1109/RADIOELEK.2016.7477386).
- [20] J. Yan, H. Hong, H. Zhao, Y. Li, C. Gu, and X. Zhu, "Through-wall multiple targets vital signs tracking based on VMD algorithm," *Sensors*, vol. 16, no. 8, p. 1293, Aug. 2016, doi: [10.3390/s16081293](https://doi.org/10.3390/s16081293).
- [21] D.-M. Chian, C.-K. Wen, F.-K. Wang, and K.-K. Wong, "Signal separation and tracking algorithm for multi-person vital signs by using Doppler radar," *IEEE Trans. Biomed. Circuits Syst.*, vol. 14, no. 6, pp. 1346–1361, Dec. 2020, doi: [10.1109/TBCAS.2020.3029709](https://doi.org/10.1109/TBCAS.2020.3029709).
- [22] H. Lv, M. Liu, T. Jiao, Y. Zhang, X. Yu, S. Li, X. Jing, and J. Wang, "Multi-target human sensing via UWB bio-radar based on multiple antennas," in *Proc. IEEE Int. Conf. IEEE Region (TENCON)*, Xi'an, China, Oct. 2013, pp. 1–4, doi: [10.1109/TENCON.2013.6718817](https://doi.org/10.1109/TENCON.2013.6718817).
- [23] J. W. Choi, D. H. Yim, and S. H. Cho, "People counting based on an IR-UWB radar sensor," *IEEE Sensors J.*, vol. 17, no. 17, pp. 5717–5727, Sep. 2017, doi: [10.1109/JSEN.2017.2723766](https://doi.org/10.1109/JSEN.2017.2723766).
- [24] E. Yavari, X. Gao, and O. Boric-Lubecke, "Subject count estimation by using Doppler radar occupancy sensor," in *Proc. 40th Annu. Int. Conf. IEEE Eng. Med. Biol. Soc. (EMBC)*, Honolulu, HI, USA, Jul. 2018, pp. 4428–4431, doi: [10.1109/EMBC.2018.8513388](https://doi.org/10.1109/EMBC.2018.8513388).
- [25] B.-K. Park, O. Boric-Lubecke, and V. M. Lubecke, "Arctangent demodulation with DC offset compensation in quadrature Doppler radar receiver systems," *IEEE Trans. Microw. Theory Techn.*, vol. 55, no. 5, pp. 1073–1079, May 2007.
- [26] C. Li and J. Lin, "Random body movement cancellation in Doppler radar vital sign detection," *IEEE Trans. Microw. Theory Techn.*, vol. 56, no. 12, pp. 3143–3152, Dec. 2008.

[27] Q. Shi, T. Zhang, G. Cui, and L. Kong, "Multi-target tracking algorithm based on multi-source clustering in distributed radar network (poster)," in *Proc. 22nd Int. Conf. Inf. Fusion (FUSION)*, Ottawa, ON, Canada, 2019, pp. 1–6.

[28] A. Kumar and A. Mukherjee, "Improvement in localization of a moving vehicle using K-means clustering," in *Proc. IEEE Int. Instrum. Meas. Technol. Conf. (IMTC)*, Dubrovnik, Croatia, May 2020, pp. 1–6, doi: [10.1109/IMTC43012.2020.9128623](https://doi.org/10.1109/IMTC43012.2020.9128623).

[29] D. Xiao, F. Su, and J. Wu, "A method of ISAR imaging for multiple targets," in *Proc. IEEE 11th Int. Conf. Signal Process.*, Beijing, China, Oct. 2012, pp. 2011–2015, doi: [10.1109/ICoSP.2012.6491975](https://doi.org/10.1109/ICoSP.2012.6491975).

[30] I. Mohammed, I. B. Collings, and S. V. Hanly, "Multiple target localization through-the-wall using non-coherent bi-static radar," in *Proc. 13th Int. Conf. Signal Process. Commun. Syst. (ICSPCS)*, Gold Coast, QLD, Australia, Dec. 2019, pp. 1–8, doi: [10.1109/ICSPCS47537.2019.9008415](https://doi.org/10.1109/ICSPCS47537.2019.9008415).

[31] Z. Yan, G. Zhang, J. Xu, T. Chen, X. Du, and J. Li, "Clustering statistic Hough transform based estimation method for motion elements of multiple underwater targets," *IEEE Access*, vol. 6, pp. 23747–23766, 2018, doi: [10.1109/ACCESS.2018.2825887](https://doi.org/10.1109/ACCESS.2018.2825887).

[32] R. Zhang and S. Cao, "Robust and adaptive radar elliptical density-based spatial clustering and labeling for mmWave radar point cloud data," in *Proc. 53rd Asilomar Conf. Signals, Syst., Comput.*, Pacific Grove, CA, USA, Nov. 2019, pp. 919–924, doi: [10.1109/IEEECONF44664.2019.9048869](https://doi.org/10.1109/IEEECONF44664.2019.9048869).

[33] J. Schlichenmaier, F. Roos, P. Hügler, and C. Waldschmidt, "Clustering of closely adjacent extended objects in radar images using velocity profile analysis," in *Proc. IEEE MTT-S Int. Conf. Microw. Intell. Mobility (ICMIM)*, Detroit, MI, USA, Apr. 2019, pp. 1–4, doi: [10.1109/ICMIM.2019.8726765](https://doi.org/10.1109/ICMIM.2019.8726765).

[34] S. Haag, B. Duraisamy, F. Govaers, W. Koch, M. Fritzsche, and J. Dickmann, "Extended object tracking assisted adaptive clustering for radar in autonomous driving applications," in *Proc. Sensor Data Fusion, Trends, Solutions, Appl. (SDF)*, Bonn, Germany, 2019, pp. 1–7, doi: [10.1109/SDF.2019.8916658](https://doi.org/10.1109/SDF.2019.8916658).

[35] K. C. Cheok, S. Nishizawa, and W. J. Young, "Moving cluster classification technique with LiDAR traffic monitoring application," in *Proc. Amer. Control Conf.*, Philadelphia, PA, USA, vol. 2, 1998, pp. 944–949, doi: [10.1109/ACC.1998.703547](https://doi.org/10.1109/ACC.1998.703547).

[36] N. Scheiner, N. Appenrodt, J. Dickmann, and B. Sick, "A multi-stage clustering framework for automotive radar data," in *Proc. IEEE Intell. Transp. Syst. Conf. (ITSC)*, Auckland, New Zealand, Oct. 2019, pp. 2060–2067, doi: [10.1109/ITSC.2019.8916873](https://doi.org/10.1109/ITSC.2019.8916873).

[37] M. Stephan and A. Santra, "Radar-based human target detection using deep residual U-Net for smart home applications," in *Proc. 18th IEEE Int. Conf. Mach. Learn. Appl. (ICMLA)*, Boca Raton, FL, USA, Dec. 2019, pp. 175–182, doi: [10.1109/ICMLA.2019.00035](https://doi.org/10.1109/ICMLA.2019.00035).

[38] M. Stolz, M. Li, Z. Feng, M. Kunert, and W. Menzel, "High resolution automotive radar data clustering with novel cluster method," in *Proc. IEEE Radar Conf. (RadarConf18)*, Oklahoma City, OK, USA, Apr. 2018, pp. 0164–0168, doi: [10.1109/RADAR.2018.8378550](https://doi.org/10.1109/RADAR.2018.8378550).

[39] S. Lim, S. Lee, and S.-C. Kim, "Clustering of detected targets using DBSCAN in automotive radar systems," in *Proc. 19th Int. Radar Symp. (IRS)*, Bonn, Germany, Jun. 2018, pp. 1–7, doi: [10.23919/IRS.2018.8448228](https://doi.org/10.23919/IRS.2018.8448228).

[40] A. G. Argüello and D. Berges, "Radar classification for traffic intersection surveillance based on micro-Doppler signatures," in *Proc. 15th Eur. Radar Conf. (EuRAD)*, Madrid, Spain, Sep. 2018, pp. 186–189, doi: [10.23919/EuRAD.2018.8546545](https://doi.org/10.23919/EuRAD.2018.8546545).

[41] M. Li, M. Stolz, Z. Feng, M. Kunert, R. Henze, and F. Küçükay, "An adaptive 3D grid-based clustering algorithm for automotive high resolution radar sensor," in *Proc. IEEE Int. Conf. Veh. Electron. Saf. (ICVES)*, Madrid, Spain, Sep. 2018, pp. 1–7, doi: [10.1109/ICVES.2018.8519483](https://doi.org/10.1109/ICVES.2018.8519483).

[42] D. Pelleg and A. W. Moore, "X-means: Extending K-means with efficient estimation of the number of clusters," in *Proc. 17th Int. Conf. Mach. Learn.*, Stanford, CA, USA, Jun. 2000, pp. 727–734.

[43] M. Mercuri, Y. Lu, S. Polito, F. Wieringa, Y.-H. Liu, A.-J. Van Der Veen, C. Van Hoof, and T. Torfs, "Enabling robust radar-based localization and vital signs monitoring in multipath propagation environments," *IEEE Trans. Biomed. Eng.*, early access, Mar. 17, 2021, doi: [10.1109/TBME.2021.3066876](https://doi.org/10.1109/TBME.2021.3066876).

[44] G. Wang, C. Gu, T. Inoue, and C. Li, "A hybrid FMCW-interferometry radar for indoor precise positioning and versatile life activity monitoring," *IEEE Trans. Microw. Theory Techn.*, vol. 62, no. 11, pp. 2812–2822, Nov. 2014, doi: [10.1109/TMTT.2014.2358572](https://doi.org/10.1109/TMTT.2014.2358572).

[45] F. Adib, H. Mao, Z. Kabelac, D. Katabi, and R. C. Miller, "Smart homes that monitor breathing and heart rate," in *Proc. 33rd Annu. ACM Conf. Hum. Factors Comput. Syst.*, New York, NY, USA, Apr. 2015, pp. 837–846.

[46] F. Adib, Z. Kabelac, and D. Katabi, "Multi-person localization via RF body reflections," in *Proc. 12th USENIX Conf. Netw. Syst. Design Implement.*, Berkeley, CA, USA, May 2015, pp. 279–292.



TAKATO KODA received the B.E. degree in electrical and electronic engineering from Kyoto University, Kyoto, Japan, in 2020. He is currently pursuing the M.E. degree in electrical engineering with the Graduate School of Engineering, Kyoto University.



TAKUYA SAKAMOTO (Senior Member, IEEE) received the B.E. degree in electrical and electronic engineering from Kyoto University, Kyoto, Japan, in 2000, and the M.I. and Ph.D. degrees in communications and computer engineering from the Graduate School of Informatics, Kyoto University, in 2002 and 2005, respectively.

From 2006 to 2015, he was an Assistant Professor with the Graduate School of Informatics, Kyoto University. From 2011 to 2013, he was a Visiting Researcher with Delft University of Technology, Delft, Netherlands. From 2015 to 2018, he was an Associate Professor with the Graduate School of Engineering, University of Hyogo, Himeji, Japan. In 2017, he was a Visiting Scholar with the University of Hawai'i at Mānoa, Honolulu, HI, USA. Since 2018, he has been a PRESTO Researcher with the Japan Science and Technology Agency, Kawaguchi, Japan. He is currently an Associate Professor with the Graduate School of Engineering, Kyoto University. His current research interests include system theory, inverse problems, radar signal processing, radar imaging, and wireless sensing of vital signs.

Dr. Sakamoto was a recipient of the Best Paper Award from the International Symposium on Antennas and Propagation (ISAP), in 2012, and the Masao Horiba Award, in 2016. In 2017, he was invited as a Semi-Plenary Speaker to the European Conference on Antennas and Propagation (EuCAP), Paris, France.



SHIGEAKI OKUMURA received the B.E. degree in electrical engineering from Kyoto University, Kyoto, Japan, in 2013, and the M.I. and Ph.D. degrees in communications and computer engineering from the Graduate School of Informatics, Kyoto University, in 2015 and 2018, respectively. He has been with MaRI Company Ltd., since 2019. His research interests include radar and audio signal processing and the non-contact measurement of vital signs.



HIROFUMI TAKI (Member, IEEE) received the M.D. and Ph.D. degrees in informatics from Kyoto University, Japan, in 2000 and 2007, respectively. He was an Assistant Professor with the Graduate School of Informatics, Kyoto University, and an Associate Professor with the Graduate School of Biomedical Engineering, Tohoku University. He founded MaRI Company Ltd., in 2017. Since 2017, he has been the CEO of MaRI Company Ltd. His research interest includes digital signal processing in measurement of biological information.

• • •